Theoret. Appl. Mech., Vol.39, No.1, pp. 27–54, Belgrade 2012

Configurational forces and shape of a sessile droplet on a rotating solid substrate

Vlado A. Lubarda* **Kurt A. Talke †**

Abstract

The shape of a uniformly rotating liquid droplet deposited on a solid substrate is determined by an iterative numerical integration of the governing nonlinear differential equation. The differential equation and the boundary conditions are derived by means of the variational analysis which delivers the expressions for the specific configurational force per unit area of the liquid/vapor interface, and the configurational force along the liquid/solid/vapor contact circle. An analytical proof for the orthogonality of the specific configurational force to the surface of the droplet is constructed. The effect of rotation on the droplet's gyrostatic shape is discussed.

Keywords: Configurational force, contact angle, droplet, Laplace pressure, line tension, rotation, surface energy, Young's equation.

1 Introduction

The study of a liquid droplet spreading over solid substrates is a fundamental problem in the mechanics of wetting, which facilitates better understanding how to modify a surface to make it more or less wettable. This is of great technological importance in the chemical industry (paints, ink, coloring ingredients), mechanical engineering (lubrication of machine parts by

*Department of Mechanical and Aerospace Engineering, University of California, San Diego; La Jolla, CA 92093-0411, USA, Montenegrin Academy of Sciences and Arts,Rista Stijovića 5, 81000 Podgorica, Montenegro, e-mail: vlubarda@ucsd.edu

†Department of Mechanical and Aerospace Engineering, University of California, San Diego; La Jolla, CA 92093-0411, USA

oils), electronics (spreading of lubricant droplets on magnetic hard disks, molten solder spreading in electronic packaging), glass industry (anti-stain or anti-frost treatments), soil and rock engineering (extraction of crude oil or water), agriculture (wettability of pesticides and herbicides), biology (rise of sap in plants, locomotion of insects on water, wetting of the eye), etc. Representative general references covering many of these topics include Zisman (1964), Rowlinson and Widom (1982), de Gennes (1985), de Gennes et al. (2004), and Miller and Neogi (2008).

The present paper is an analytical and numerical determination of the equilibrium shape of a uniformly rotating liquid droplet deposited on a flat solid substrate. The study is based on the variational approach and mechanics of configurational forces. The utilized variational analysis has been previously used by Johnson (1959), Blokhuis et al. (1995), Bormashenko and Whyman (2008), Whyman et al. (2008), Blokhius (2005), and Bormashenko (2009), and has its roots in general Gibbs thermodynamics (Gibbs, 1961). Particular attention in these papers was given to the variational proof of the independence of the wetting contact angle on the gravity field. This is extended in the present paper to include the contact angle independence from the angular speed of rotation. The numerical determination of the droplet's shape is performed by an iterative solution of the governing nonlinear differential equation, similar to the iterative procedure used to determine the shape of a nonrotating liquid droplet (Padday, 1991; Blokhuis, 2005).

The analysis of a droplet's spreading within the framework of configurational forces was previously employed by Gao et al. (2000), Fan et al. (2001), and Fan (2006), who studied molten solder spreading in electronic packaging. Configurational forces were used to circumvent, to some extent, the complexities associated with a detailed fluid mechanics solution of the spreading process (Dussan, 1979; Ehrhard and Davis, 1991; Li et al., 2010). A general study of the configurational forces in mechanics can be found in review articles by Maugin (1995) and Suo (1997), and in the monograph by Gurtin (2000). Configurational (material or energetic) forces are important for the kinetic study of numerous problems of materials science, in which the relevant velocity is assumed to depend on the corresponding configurational force. For example, in dislocation theory the velocity of a dislocation segment is a function of the Peach-Koehler force acting on that segment (Hirth and Lothe, 1982). In crystalline plasticity the rate of crystallographic slip is a function of the resolved shear stress of that slip system (Asaro and

Lubarda, 2005), while in fracture mechanics the velocity of the crack tip is a function of the free-energy reduction associated with the advancement of the crack tip (Freund, 1990).

In this paper we derive the expression for the configurational force acting on a three-phase (liquid/solid/vapor) contact circle in terms of the surface and line tensions, the volume of the droplet, and the contact angle between the droplet and substrate. In the gyrostatic configuration, this configurational force vanishes, which yields the Boruvka–Neumann equation (Boruvka and Neumann, 1977), or the Young's equation if the line tension effect is omitted (Young, 1805). The specific configurational force, per unit area of the liquid/vapor interface, is also derived, which is the difference between the gravity and rotation dependent Laplace pressure and curvature scaled surface tension. An analytical proof for the orthogonality of the specific configurational force to the surface of the droplet is constructed. The effect of rotation on the droplet's gyrostatic shape is then discussed.

2 Variational analysis of a droplet spreading

Consider a liquid droplet slowly (quasistatically) spreading toward its equilibrium configuration on a flat, smooth solid substrate, that is rotating with a constant angular speed ω. Under constant ambient pressure and temperature, the effective mechanical potential (Lamb, 1932; Lytletton, 1953) of the system is

$$L = U - K\,, \tag{1}$$

where

$$U = \sigma_{lv}S + (\sigma_{sl} - \sigma_{sv})R^2\pi + 2\pi R\tau + \int_0^h (\Delta\gamma)z\,\mathrm{d}V \tag{2}$$

is the free energy, and

$$K = \int_V k(\varrho)\,\mathrm{d}V = 2\pi\int_0^h \mu(r)\,\mathrm{d}z\,, \quad \mu(r) = \frac{1}{8}\,\rho_l\omega^2 r^4 \tag{3}$$

is the kinetic energy of the droplet. The specific weight difference is $\Delta\gamma = \gamma_l - \gamma_v = (\rho_l - \rho_v)g$, where ρ denotes density and g denotes gravitational acceleration. Thus, the last term on the right-hand side of (3) represents gravitational potential energy. The liquid volume element is $\mathrm{d}V = r^2(z)\pi\,\mathrm{d}z$,

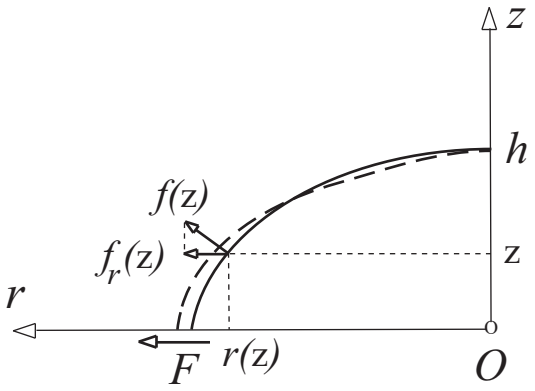

Figure 1: The virtual displacement imposed in the horizontal (r) direction takes the surface of the droplet from its solid- to dashed-line configuration. The corresponding configurational forces are F and f_r.

and the radius $R = r(0)$. The kinetic energy density k is defined by

$$k(\varrho) = \frac{1}{2}\,\rho_l \varrho^2 \omega^2\,, \quad \varrho \in [0, r]\,. \tag{4}$$

The scaled kinetic energy density $\mu(r)$ is introduced for convenience, and is related to k by $\mu(r) = r^2 k(r)/4$. The surface S in (2) is the surface of the axisymmetric liquid/vapor interface whose profile $r = r(z)$ is to be determined. The solid/vapor and liquid/vapor surface energies are denoted by σ_{sv} and σ_{lv}, the solid/liquid interface energy by σ_{sl}, and τ is the line tension along the triple solid/liquid/vapor contact line. The expression for the surface S is

$$S = \int_0^h 2\pi r(z)\,\mathrm{d}s\,, \quad \mathrm{d}s = [1 + r'^2(z)]^{1/2}\,\mathrm{d}z\,. \tag{5}$$

In the sequel, it will be assumed there is no evaporation of liquid during the spreading of the droplet, so that its volume remains constant. The appropriate functional for the variational study is then

$$\Pi = L - \lambda V\,, \quad V = \int_0^h r^2(z)\pi\,\mathrm{d}z\,, \tag{6}$$

where λ is the Lagrangian multiplier, with dimension of pressure. In view of (2)–(5), the potential function Π in (6) can be written as

$$\Pi = \int_0^h \Phi(z, r, r')\,\mathrm{d}z\,, \tag{7}$$

where

$$\begin{aligned}\Phi = {} & \sigma_{lv} 2\pi r(z)[1 + r'^2(z)]^{1/2} - r^2(z)\pi(\lambda - z\Delta\gamma) - 2\pi\mu(r) \\ & + \frac{1}{h}\left[(\sigma_{sl} - \sigma_{sv})r^2(z)\pi + 2\pi r(z)\tau\right]\bar{\delta}(z)\,.\end{aligned} \tag{8}$$

The Dirac delta function $\bar{\delta}(z)$ is here defined such that $\int_0^h r(z)\bar{\delta}(z)\,\mathrm{d}z = hr(0)$, because z has a dimension of the length h (height of the droplet). Following the well-known derivation from Euler-Lagrange's variational calculus, the variation of the potential functional $\delta\Pi$, divided by the corresponding infinitesimal variation $\delta r(z)$ of the shape function $r = r(z)$, at an arbitrary $z = \zeta$, is

$$\frac{\delta\Pi}{\delta r(\zeta)} = h\left[\frac{\partial\Phi}{\partial r} - \frac{\mathrm{d}}{\mathrm{d}z}\left(\frac{\partial\Phi}{\partial r'}\right)\right]_{z=\zeta} + \left[\frac{\partial\Phi}{\partial r'}\,\bar{\delta}(z-\zeta)\right]_{z=0}^{z=h}\,. \tag{9}$$

The first term on the right-hand side has the usual form of Euler-Lagrange's differential equation, while the second term accounts for boundary conditions. From (8), it readily follows that

$$\begin{aligned}\frac{\partial\Phi}{\partial r} = {} & 2\pi\left[\sigma_{lv}(1 + r'^2)^{1/2} - r(\lambda - z\Delta\gamma) - \frac{\partial\mu}{\partial r}\right] \\ & + \frac{2\pi}{h}\left[R(\sigma_{sl} - \sigma_{sv}) + \tau\right]\bar{\delta}(z)\,,\end{aligned} \tag{10}$$

$$\frac{\partial\Phi}{\partial r'} = 2\pi\sigma_{lv}\,\frac{rr'}{(1 + r'^2)^{1/2}}\,, \tag{11}$$

$$\frac{\mathrm{d}}{\mathrm{d}z}\left(\frac{\partial\Phi}{\partial r'}\right) = 2\pi\sigma_{lv}\left[(1 + r'^2)^{1/2} - 2r\kappa\right]\,. \tag{12}$$

The mean curvature of the droplet's profile is $\kappa = (\kappa_1 + \kappa_2)/2$, and

$$\kappa_1 = \frac{1}{r(1 + r'^2)^{1/2}}\,, \quad \kappa_2 = -\frac{r''}{(1 + r'^2)^{3/2}} \tag{13}$$

are its two principal curvatures. Furthermore, in view of (11),

$$\left[\frac{\partial \Phi}{\partial r'}\,\bar{\delta}(z-\zeta)\right]_{z=0}^{z=h} = 2\pi R\sigma_{lv}\cos\theta_0\bar{\delta}(\zeta)\,, \tag{14}$$

because the slope at the apex of the droplet $r'(h)$ vanishes by symmetry, and the cosine of angle θ_0 between the tangent to the droplet's profile and horizontal surface of the substrate is

$$\cos\theta_0 = -\frac{r'(0)}{[1+r'^{\,2}(0)]^{1/2}}\,. \tag{15}$$

Consequently, by substituting (10), (12), and (14) into (9), and noting that $rk = \partial\mu/\partial r$, we obtain

$$\begin{aligned}\frac{\delta\Pi}{\delta r(\zeta)} &= 2\pi h r(\zeta)\,[2\sigma_{lv}\kappa(\zeta) - \lambda + \zeta\Delta\gamma - k(r)] \\ &\quad + 2\pi R\left(\sigma_{lv}\,\cos\theta_0 + \sigma_{sl} - \sigma_{sv} + \frac{\tau}{R}\right)\,\bar{\delta}(\zeta)\,,\end{aligned} \tag{16}$$

where $k(r)$ is the kinetic energy density at the droplet surface, defined by (4).

2.1 Configurational forces

The configurational force (F) per unit length of the three-phase (liquid/ solid/ vapor) contact circle, and the specific configurational force ($\mathbf{f}$) per unit area of the liquid/vapor interface are defined such that

$$-\delta\Pi = \int_0^h 2\pi r(z) f_r(z)\delta r(z)\,\mathrm{d}s + 2\pi R F\delta R\,, \tag{17}$$

where $\mathbf{f}(z)\cdot\delta\mathbf{r}(z) = f_r(z)\,\delta r(z)$, so that $f_r(z)$ is the projection of $\mathbf{f}$ onto the horizontal direction of the virtual displacement $\delta r(z)$ (Fig.1). The direction of $\mathbf{f}(z)$ is unspecified at this stage of analysis, although it will be shown in section 4 that it is orthogonal to the droplet surface.[1] By dividing this with the shape variation $\delta r(\zeta)$, we find

$$-\frac{\delta\Pi}{\delta r(\zeta)} = 2\pi h r(\zeta)(1+r'^{\,2})^{1/2}\,f_r(\zeta) + 2\pi R\,F\,\bar{\delta}(\zeta)\,. \tag{18}$$

[1] Physically, this orthogonality is anticipated from the outset, because the component of the configurational force tangential to the surface of the droplet does not affect the shape of the surface, and thus can be taken to be zero.

Through comparing (16) and (18), we deduce the expressions for the configurational forces

$$f_r(\zeta) = \frac{1}{[1 + r'^2(\zeta)]^{1/2}} \left[\lambda - 2\sigma_{lv}\kappa(\zeta) - \zeta\Delta\gamma + k(r)\right], \tag{19}$$

and

$$F = \sigma_{sv} - \sigma_{sl} - \sigma_{lv}\cos\theta_0 - \frac{\tau}{R}. \tag{20}$$

To determine an expression for the Lagrangian multiplier λ, we impose the condition $f_r(h) = 0$, which holds by the symmetry of the droplet around its vertical axis through the apex of the droplet ($z = h$). Locally, at the apex, the surface of the droplet is a sphere, say of radius b, so that $\kappa = \kappa_1 = \kappa_2 = 1/b$ at $\zeta = h$, we obtain, from (19),

$$\lambda = \frac{2}{b}\,\sigma_{lv} + h\Delta\gamma. \tag{21}$$

The substitution of (21) into (19) thus yields

$$f_r(\zeta) = \frac{1}{[1 + r'^2(\zeta)]^{1/2}} \left\{2\sigma_{lv}\left[\frac{1}{b} - \kappa(\zeta)\right] + (\Delta\gamma)(h - \zeta) + k(r)\right\}. \tag{22}$$

2.2 Equilibrium configuration

In the equilibrium configuration of the droplet, its configurational forces vanish ($F = 0$ and $f = 0$), so that (20) gives a modified Young's equation (incorporating the line tension τ), also known as the Boruvka–Neumann equation (Boruvka and Neumann, 1977; Widom, 1995)

$$\cos\theta_0 = \frac{\sigma_{sv} - \sigma_{sl}}{\sigma_{lv}} - \frac{\tau}{R}, \tag{23}$$

while (22) yields a modified Laplace–Young's equation (incorporating the external field μ)

$$2\sigma_{lv}\left(\kappa - \frac{1}{b}\right) = (\Delta\gamma)(h - \zeta) + k(r). \tag{24}$$

In view of the curvature expressions (13), we can rewrite (24) as

$$\frac{1}{r(1 + r'^2)^{1/2}} - \frac{r''}{(1 + r'^2)^{3/2}} = \frac{\Delta\gamma}{\sigma_{lv}}\,(h - \zeta) + \frac{2}{b} + \frac{k(r)}{\sigma_{lv}}, \tag{25}$$

which reduces to the well-known Laplace's equation in the absence of rotation.

In the case of a spherical droplet model (i.e., zero gravity and no rotation), Laplace's equation gives $2(\sigma_{lv}/b) = \Delta p$. When this is applied locally to the spherical top portion of the rotating droplet in the gravity field, we can write $2(\sigma_{lv}/b) = \Delta p(h)$. Consequently, in the equilibrium state of the droplet, the Lagrangian multiplier λ in equation (21) can be interpreted as the pressure difference between the liquid and vapor phase at $z = 0$, i.e., $\lambda = \Delta p(0) = \Delta p(h) + h\Delta\gamma$.

2.3 Numerical integration

The numerical integration of (25) proceeds in an iterative semi-inverse fashion. In doing so, it is convenient to place the coordinate origin at the top or apex of the droplet, with the coordinates (z, r) as in Fig.2, so that (25) becomes

$$\frac{1}{r(1+r'^2)^{1/2}} - \frac{r''}{(1+r'^2)^{3/2}} = \frac{2}{b} + \frac{\Delta\gamma}{\sigma_{lv}}\, z + \frac{1}{2}\,\frac{\rho_l \omega^2}{\sigma_{lv}}\, r^2 \,. \tag{26}$$

The ratio $\sigma_{lv}/\Delta\gamma$ is the square of the capillary length (e.g., de Gennes et al., 2004). The integration proceeds by assuming the value of the unknown radius b, integrating (26) until the slope r' matches the angle θ_0, calculated from (23), i.e., $r'(h) = \cot\theta_0$. The boundary conditions at the origin are $r(0) = 0$ and infinite slope $r'(0)$. The integration specifies the height h, corresponding to the assumed value of b, and the matched slope $r'(h)$. The obtained solution is then the solution of the problem for a droplet which has volume corresponding to the calculated $r = r(z)$ and h. In the nonrotating droplet case ($\mu = 0$), the tabulated results are available for different values of b and V (Bashforth and Adams, 1893; Padday, 1969,1991; Blokhuis, 2005).

The nondimensional version of (26) is

$$\frac{1}{\bar{r}(1+\bar{r}'^2)^{1/2}} - \frac{\bar{r}''}{(1+\bar{r}'^2)^{3/2}} = 2 + B_0\bar{z} + \frac{1}{2}\,B_\omega \bar{r}^2 \,. \tag{27}$$

where

$$B_0 = \frac{b^2\Delta\gamma}{\sigma_{lv}}\,, \quad B_\omega = \frac{b^2\rho_l(b\omega^2)}{\sigma_{lv}} \tag{28}$$

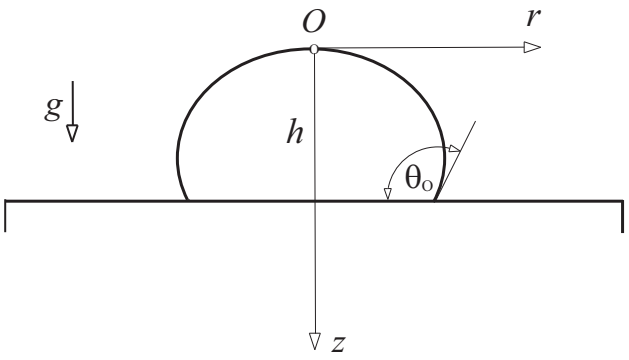

Figure 2: The equilibrium shape of a liquid droplet deposited on a flat substrate in the gravity field g. The equilibrium contact angle is θ_0 and the height of the droplet is h. The coordinate origin O is at the apex of the droplet.

are the gravitational and rotational Bond numbers, and $\bar{r} = r/b$, $\bar{z} = z/b$. Figure 3 shows a water droplet's shape in the case when $B_\omega = 0$ (non-rotating droplet), and $B_\omega = 15$. The gravitational Bond numbers are $B_0 = 5$ and $B_0 = 10$. These values were numerically adjusted by an iterative procedure so that the volume of the droplet in both cases is the same $V = 46.5$ mm^3. The solid substrate was selected so that the equilibrium wetting contact angle is $\theta_0 = 56^\circ$. The capillary length of water (surrounded by air) is $l = 2.73$ mm. The radii of curvature at the top of the droplet ($b = B_0^{1/2} l$) were therefore $b = 6.1045$ mm and 8.633 mm, respectively. The calculated droplet's heights are $h = 1.7398$ mm and 1.5583 mm, while the radii of the contact circle with the substrate are $R = 3.8718$ mm and 4.0191 mm.

Figure 4 shows the water droplet's shape in the case $B_\omega = 0$ and $B_\omega = 18.576$. The gravitational Bond numbers are $B_0 = 10$ and $B_0 = 20$. Again, these values were numerically adjusted by an iterative procedure so that the volume of the droplet in both cases is the same $V = 275$ mm^3. The solid substrate was selected so that the equilibrium wetting contact angle is $\theta_0 = 122^\circ$. The radii of curvature at the top of the droplet ($b = B_0^{1/2} l$) were therefore $b = 8.633$ mm and 12.209 mm, respectively. The calculated droplet's heights are $h = 4.417$ mm and 3.933 mm, while the radii of the contact circle with the substrate are $R = 4.993$ mm and 5.208 mm. The maximum lateral spread of the droplet in the two cases are $r_{\max} = 5.252$

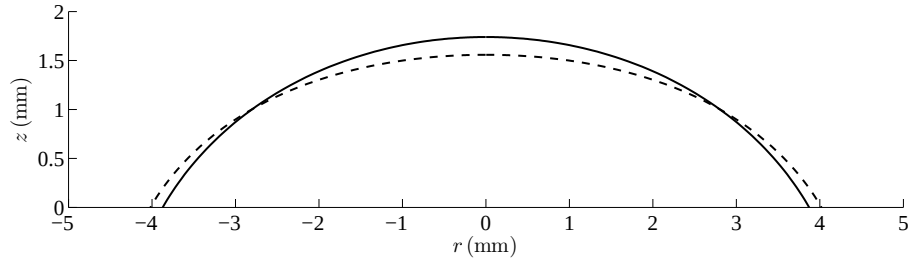

Figure 3: The equilibrium shape of a water droplet deposited on a flat substrate in the gravity field. Solid line is for a non-rotating droplet and the dashed line is for a uniformly rotating droplet, as described in the text. The contact angle with the substrate is $\theta_0 = 56^\circ$.

mm and 5.444 mm.

In both cases shown in Figs.3 and 4, the centrifugal forces cause an increase of the droplet's spreading, i.e., an increase of the radius of the contact circle and a lowering of the height of the droplet, compared to unrotating droplet shapes. In the case of a hydrophobic contact ($\theta_0 > 90^\circ$), shown in Fig. 4, the maximum width of the droplet, which occurs at some distance above the substrate, also increases by the rotation. The equilibrium droplets' shapes shown in Figs.3 and 4 are close to ellipsoidal (oblate spheroid) shapes. The range of validity of the ellipsoidal approximation of a droplet's shape has been recently examined by Lubarda and Talke (2011).

3 Variational analysis with virtual displacements in the radial direction

Since $z = \rho\cos\varphi$ and $r = \rho\sin\varphi$, the height of the droplet is $h = \rho(0)$, while the radius of the solid/liquid contact circle is $R = \rho(\pi/2)$. Furthermore, $\mathrm{d}z = (\rho' c - \rho s)\,\mathrm{d}\varphi$, where, for brevity, the abbreviations $s = \sin\varphi$ and $c = \cos\varphi$ are introduced. We note that $\rho' c - \rho s < 0$, because, for the selected orientation of the z-axis, $\mathrm{d}z < 0$ for $\mathrm{d}\varphi > 0$. The Lagrangian of the system is

$$L = \sigma_{sv} S + (\sigma_{sl} - \sigma_{sv}) R^2 \pi + 2\pi R\tau + U - K\,, \quad R = \rho(\pi/2)\,. \tag{29}$$

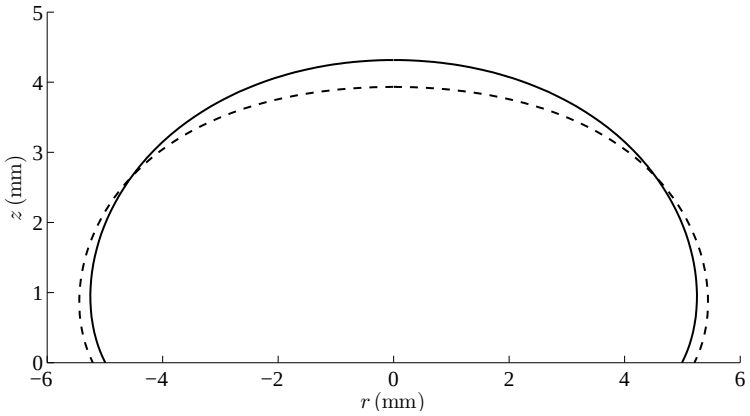

Figure 4: The equilibrium shape of a water droplet deposited on a flat substrate in the gravity field. Solid line is for a non-rotating droplet and the dashed line is for a uniformly rotating droplet, as described in the text. The contact angle with the substrate is $\theta_0 = 122^\circ$.

The surface area of the liquid/vapor interface can be determined from

$$S = \int_0^{\pi/2} 2\pi\rho(\rho^2 + \rho'^2)^{1/2} s \, \mathrm{d}\varphi \,, \tag{30}$$

while the potential energy due to gravity is

$$U = \pi(\Delta\gamma) \int_0^{\pi/2} \rho^3(\rho s - \rho' c) s^2 c \, \mathrm{d}\varphi \,. \tag{31}$$

The kinetic energy is

$$K = 2\pi \int_0^{\pi/2} \hat{\mu}(\rho, \varphi)(\rho s - \rho' c) \, \mathrm{d}\varphi \,, \quad \hat{\mu} = \frac{1}{8} \rho_l \omega^2 \rho^4 s^4 \,. \tag{32}$$

If there is no evaporation of the droplet during spreading, so that its volume remains constant, the appropriate potential for the variational study is

$$\Pi = L - \lambda V \,, \quad V = \pi \int_0^{\pi/2} \rho^2 s^2 (\rho s - \rho' c) \, \mathrm{d}\varphi \,, \tag{33}$$

where λ is the Lagrangian multiplier, with dimension of pressure. In view of (29)–(33), the potential function Π in (33) can be written as

$$\Pi = \int_0^{\pi/2} \hat{\Phi}(\rho, \rho', \varphi)\, \mathrm{d}\varphi\,, \tag{34}$$

where

$$\begin{aligned} \hat{\Phi} &= \sigma_{lv} 2\pi s\rho[\rho^2 + \rho'^2]^{1/2} + \pi\rho^2(\rho s - \rho' c)s^2(\rho c\Delta\gamma - \lambda) \\ &\quad - 2\pi(\rho s - \rho' c)\hat{\mu}(\rho, \varphi) \\ &\quad + \pi\rho\left[(\sigma_{sl} - \sigma_{sv})\rho + 2\tau\right]\bar{\delta}(\varphi - \pi/2)\,. \end{aligned} \tag{35}$$

The variation of the potential functional $\delta\Pi$, divided by the corresponding infinitesimal variation $\delta\rho(\psi)$ of the shape function $\rho = \rho(\varphi)$, at an arbitrary angle $\varphi = \psi$, is

$$\frac{\delta\Pi}{\delta\rho(\psi)} = \left[\frac{\partial\hat{\Phi}}{\partial\rho} - \frac{\mathrm{d}}{\mathrm{d}\varphi}\left(\frac{\partial\hat{\Phi}}{\partial\rho'}\right)\right]_{\varphi=\psi} + \left[\frac{\partial\hat{\Phi}}{\partial\rho'}\,\bar{\delta}(\varphi - \psi)\right]_{\varphi=0}^{\varphi=\pi/2}\,. \tag{36}$$

From (35) it readily follows that

$$\begin{aligned} \frac{\partial\hat{\Phi}}{\partial\rho} &= 2\pi\left[\sigma_{lv} s\,\frac{2\rho^2 + \rho'^2}{(\rho^2 + \rho'^2)^{1/2}} - \frac{\partial\hat{\mu}}{\partial\rho}\,(\rho s - \rho' c) - \hat{\mu} s\right] \\ &\quad + (\Delta\gamma)\pi\rho^2 s^2 c(4\rho s - 3\rho' c) - \lambda\pi\rho s^2(3\rho s - 2\rho' c) \\ &\quad + 2\pi\left[(\sigma_{sl} - \sigma_{sv})R + \tau\right]\bar{\delta}(\varphi - \pi/2)\,, \end{aligned} \tag{37}$$

$$\frac{\partial\hat{\Phi}}{\partial\rho'} = 2\pi\left[\sigma_{lv} s\,\frac{\rho\rho'}{(\rho^2 + \rho'^2)^{1/2}} + \hat{\mu} c\right] - \pi\rho^2 c s^2\left[(\Delta\gamma)\rho c - \lambda\right], \tag{38}$$

$$\begin{aligned} \frac{\mathrm{d}}{\mathrm{d}\varphi}\left(\frac{\partial\hat{\Phi}}{\partial\rho'}\right) &= 2\pi\left\{\sigma_{lv} s\left[\frac{2\rho^2 + \rho'^2}{(\rho^2 + \rho'^2)^{1/2}} - 2\kappa\rho^2\right] - \hat{\mu} s + \left(\frac{\partial\hat{\mu}}{\partial\rho}\,\rho' + \frac{\partial\hat{\mu}}{\partial\varphi}\right) c\right\} \\ &\quad - (\Delta\gamma)\pi\rho^2 sc[3\rho' sc + 2\rho(c^2 - s^2)] + \lambda\pi\rho s[2\rho' sc + \rho(2c^2 - s^2)]\,. \end{aligned} \tag{39}$$

The mean curvature of the droplet's profile is $\kappa = (\kappa_1 + \kappa_2)/2$, and

$$\kappa_1(\varphi) = \frac{1}{\rho s}\,\frac{\rho s - \rho' c}{(\rho^2 + \rho'^2)^{1/2}}\,, \quad \kappa_2(\varphi) = \frac{\rho^2 + 2\rho'^2 - \rho\rho''}{(\rho^2 + \rho'^2)^{3/2}} \tag{40}$$

are its two principal curvatures. Furthermore, in view of (38),

$$\left[\frac{\partial\hat{\Phi}}{\partial\rho'}\,\bar{\delta}(\varphi-\psi)\right]_{\varphi=0}^{\varphi=\pi/2} = 2\pi R\sigma_{lv}\cos\theta_0\bar{\delta}(\psi-\pi/2)\,, \tag{41}$$

because the slope at the apex of the droplet $\rho'(0)$ vanishes by symmetry, and the cosine of the angle θ between the tangent to the droplet's profile and the horizontal surface of the substrate is

$$\cos\theta_0 = \frac{\rho'(\pi/2)}{[\rho^2(\pi/2)+\rho'^2(\pi/2)]^{1/2}}\,. \tag{42}$$

Consequently, by substituting (37), (39), and (41) into (36), we obtain

$$\begin{aligned}\frac{\delta\Pi}{\delta\rho(\psi)} &= 2\pi\rho^2\sin\psi[2\sigma_{lv}\kappa(\psi)+(\Delta\gamma)\rho\cos\psi-\lambda]\\ &\quad -2\pi\rho\left(\frac{\partial\hat{\mu}}{\partial\rho}\,\sin\psi+\frac{1}{\rho}\,\frac{\partial\hat{\mu}}{\partial\psi}\,\cos\psi\right)\\ &\quad +2\pi R\big(\sigma_{lv}\,\cos\theta+\sigma_{sl}-\sigma_{sv}+\frac{\tau}{R}\big)\,\bar{\delta}(\psi-\pi/2)\,.\end{aligned} \tag{43}$$

3.1 Configurational forces

The configurational force (F) per unit length of the three-phase contact circle, and the specific configurational force ($\mathbf{f}$), per unit area of the liquid/vapor interface, are defined such that

$$-\delta\Pi = \int_0^{\pi/2} 2\pi s\rho(\rho^2+\rho'^2)^{1/2}f_\rho(\varphi)\;\delta\rho(\varphi)\,\mathrm{d}\varphi + 2\pi RF\delta R\,, \tag{44}$$

where $\mathbf{f}(\varphi)\cdot\delta\boldsymbol{\rho}(\varphi) = f_\rho(\varphi)\delta\rho_(\varphi)$, so that $f_\rho(\varphi)$ is the projection of $\mathbf{f}(\varphi)$ on the radial direction of the virtual displacement $\delta\boldsymbol{\rho}(\varphi)$ (Fig.3). By dividing (44) by the variation $\delta\rho(\psi)$, there follows

$$-\frac{\delta\Pi}{\delta\rho(\psi)} = 2\pi\sin\psi\rho(\rho^2+\rho'^2)^{1/2}\,f_\rho(\psi)+2\pi RF\bar{\delta}(\psi-\pi/2)\,, \tag{45}$$

with $\rho=\rho(\psi)$.

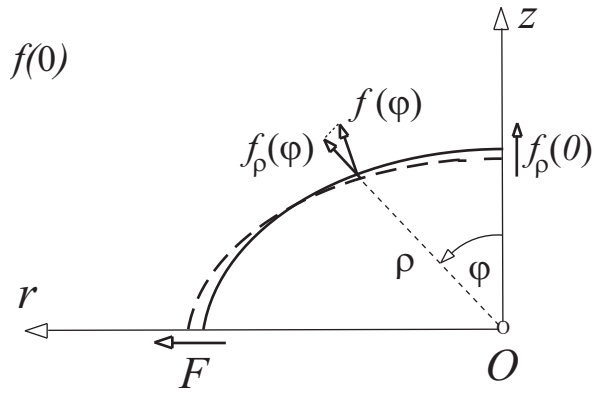

Figure 5: The virtual displacement imposed in the radial (ρ) direction takes the surface of the droplet from its solid- to dashed-line configuration. The corresponding configurational forces are F and f_ρ.

By comparing (43) and (45), we deduce the following expressions for the configurational forces

$$f_\rho = \frac{\rho}{(\rho^2+\rho'^2)^{1/2}}\left[\lambda - 2\sigma_{lv}\kappa(\psi) - (\Delta\gamma)\rho\cos\psi + \frac{1}{\rho}\left(\frac{\partial\hat{\mu}}{\partial\rho} - \frac{1}{\rho}\,\frac{\partial\hat{\mu}}{\partial\psi}\,\cot\psi\right)\right], \tag{46}$$

$$F = \sigma_{sv} - \sigma_{sl} - \sigma_{lv}\cos\theta_0 - \frac{\tau}{R}\,. \tag{47}$$

The expression (47) is the same as expression (17) from section 2. Regarding expression (46), it is first observed that

$$k = \frac{1}{r}\,\frac{\partial\mu}{\partial r} = \frac{1}{\rho}\left(\frac{\partial\hat{\mu}}{\partial\rho} + \frac{1}{\rho}\,\frac{\partial\hat{\mu}}{\partial\varphi}\,\cot\varphi\right) = \frac{1}{2}\,\rho_l\omega^2\rho^2\sin^2\varphi\,, \tag{48}$$

which can be verified by inspection from $\mu(r) = \hat{\mu}(\rho,\varphi)$, $r = \rho\sin\varphi$, and $z = \rho\cos\varphi$. Next, by symmetry, the droplet's shape at $\psi = 0$ is locally a sphere.[2]. The configurational force on a spherical expansion of a spherical droplet (no gravity), is $f = \Delta p - 2\sigma_{lv}/b$, where Δp is the pressure difference

[2]In the terminology of differential geometry, the apex of the droplet is a navel point of its bounding surface.

across the surface of the droplet, and b the radius of the droplet.[3] We now reconcile this expression with the expression for $f_\rho(0)$, following from (46) when $\psi = 0$. Since $\rho'(0) = 0$, $\kappa_1(0) = \kappa_2(0) = 1/b$, and $\rho(0) = h$ (the height of the droplet), we have

$$\lambda - \frac{2}{b}\,\sigma_{lv} - h\Delta\gamma = \Delta p(0) - \frac{2}{b}\,\sigma_{lv}\,. \tag{49}$$

Thus, the Lagrangian multiplier λ can be expressed as

$$\lambda = \Delta p(0) + h\Delta\gamma\,, \tag{50}$$

i.e., it can be interpreted as the pressure difference between the liquid and vapor interface at the bottom of the droplet: $\lambda = \Delta p(\pi/2) = \Delta p(0) + h\Delta\gamma$. The substitution of (48) and (50) into (46) thus yields

$$f_\rho = \frac{\rho}{(\rho^2 + \rho'^{\,2})^{1/2}}\,[-2\sigma_{lv}\kappa + (\Delta\gamma)(h - \rho\cos\psi) + \Delta p(0) + k]\,. \tag{51}$$

In the equilibrium configuration of the droplet, its configurational forces vanish ($F = 0$ and $f_\rho = 0$), so that (47) gives a modified Young's equation (22), while (51) yields a modified Laplace–Young's equation

$$2\sigma_{lv}\left(\kappa - \frac{1}{b}\right) = (\Delta\gamma)(h - \rho\cos\psi) + k\,, \tag{52}$$

because in the equilibrium configuration $\Delta p(0) = 2\sigma_{lv}/b$.

4 Orthogonality of the specific configurational force to the surface of the droplet

From the results presented in sections 2 and 3, it can now be proven that the specific configurational force $\mathbf{f}$ is orthogonal to the surface of the droplet. To that goal, it is first observed that

$$\left(\frac{\rho^2 + \rho'^{\,2}}{1 + r'^{\,2}}\right)^{1/2} = \rho\sin\varphi - \rho'\cos\varphi\,, \tag{53}$$

[3] Because, in this case the potential energy is $\Pi = \sigma_{lv}S - (\Delta p)V$, where $S = 4\pi b^2$ and $V = (4\pi/3)b^3$, and by defining f such that $4\pi b^2 f = -\partial\Pi/\partial b$, there follows the result.

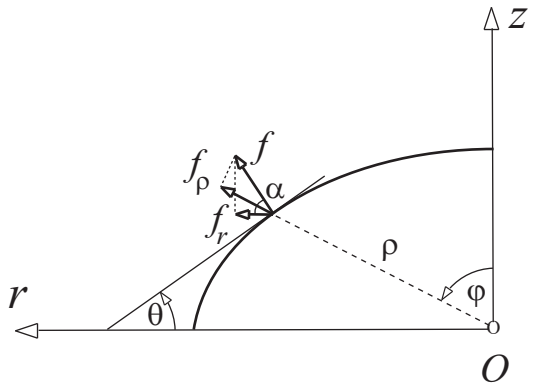

Figure 6: The specific configuration force f is orthogonal to the surface of the droplet. Its components in the r and ρ directions are f_r and f_ρ, respectively. The tangent line to the surface of the droplet makes the angle θ with the horizontal direction.

so that, from (22) and (45),

$$\frac{f_r}{f_\rho} = \sin\varphi - \frac{\rho'}{\rho}\cos\varphi\,. \tag{54}$$

Denoting by α the angle between $\mathbf{f}$ and $\mathbf{f}_r$ (Fig. 6), $f_r = f\cos\alpha$ and $f_\rho = f\sin(\alpha+\varphi)$, which can be rewritten as

$$f\cos\alpha = f_r\,, \quad f\sin\alpha = \frac{f_\rho}{\cos\varphi} - f_r\tan\varphi\,. \tag{55}$$

By dividing the last two expressions, and by using (54) to eliminate the ratio f_ρ/f_r, there follows

$$\tan\alpha = \frac{\cos\varphi + (\rho'/\rho)\sin\varphi}{\sin\varphi - (\rho'/\rho)\cos\varphi}\,. \tag{56}$$

From Fig. 6, the ratio $(\rho'/\rho) = \tan(\varphi-\theta)$, which can be rewritten as

$$\frac{\rho'}{\rho} = \frac{\tan\varphi - \tan\theta}{1+\tan\varphi\tan\theta}\,, \tag{57}$$

where θ is the angle between the tangent to the curve $\rho = \rho(\varphi)$ and the horizontal direction, as indicated in Fig.6. Consequently, by substituting

(57) into (56),

$$\tan\alpha = \frac{1}{\tan\theta}\,, \tag{58}$$

meaning that $\alpha = \pi/2 - \theta$, so that the configurational force $\mathbf{f}$ is indeed orthogonal to the surface of the droplet, at any point on its surface S. The magnitude of this force follows from (55) as

$$f = \frac{1}{\sin\theta}\, f_r\,, \tag{59}$$

where f_r is specified by (22). Thus,

$$f(z) = 2\sigma_{lv}\left[\frac{1}{b} - \kappa(z)\right] + (\Delta\gamma)(h-z) + \frac{1}{2}\,\rho_l r^2\omega^2\,. \tag{60}$$

This can be interpreted as

$$f(z) = \Delta p - 2\sigma_{lv}\kappa(z)\,, \tag{61}$$

where the rotation-dependent Laplace's pressure is

$$\Delta p = 2\frac{\sigma_{lv}}{b} + (\Delta\gamma)(h-z) + \frac{1}{2}\,\rho_l r^2\omega^2\,. \tag{62}$$

Returning to the components of the specific configurational force, it is also noted that, from (54) and (57), their ratio is

$$\frac{f_\rho}{f_r} = \sin\varphi + \cos\varphi\cot\theta\,. \tag{63}$$

5 Conclusions

The shape of a uniformly rotating liquid droplet in the gravity field was determined by numerical integration of the governing nonlinear differential equation. This was accomplished by using an iterative procedure, commonly used to determine the shape of a nonrotating droplet. The effect of rotation on the gyrostatic shape of the droplet was discussed. The governing differential equation and the accompanying boundary conditions were derived by means of a variational analysis which delivers the expressions for configurational forces acting on the surface of the droplet and along the three-phase contact circle. The specific configurational force per unit area of

the liquid/vapor interface is the difference between the gravity and rotation dependent Laplace pressure and the curvature scaled surface tension. The configurational force along the liquid/solid/vapor contact circle depends on the involved surface and line tensions, the volume of the droplet, and the contact angle between the droplet and the solid substrate, but not on the droplet's specific weight or the angular speed of rotation. The utilized variational procedure is based on the infinitesimal variation of a droplet's shape imposed in the horizontal direction, parallel to the surface of the substrate. An alternative derivation was then constructed, based on the displacement variations along the radii from the center of the solid/liquid interface circle. By comparing the results from these two derivations, it was proven that the specific configurational force is orthogonal to the liquid/vapor interface, as physically expected. The effect of rotation on the droplet's gyrostatic shape was discussed.

Acknowledgment: This research was supported by the Montenegrin Academy of Sciences and Arts and by the MAE endowment fund at UCSD. Valuable discussions with Professor Frank E. Talke on the mechanics of wetting phenomena and with Professor Xanthippi Markenscoff on the mechanics of configurational forces are also acknowledged.

References

[1] Asaro, R.J., Lubarda, V.A., 2005. Mechanics of Solids and Materials. Cambridge University Press, New York.

[2] Bashforth, F., Adams, J.C., 1893. An Attempt to Test the Theory of Capillary Action. Cambridge University Press, Cambridge.

[3] Blokhuis, E.M., 2005. Liquid drops at surfaces. In: Surface and Interfacial Tension: Measurement, Theory, and Applications, Surfactant Science Series, Vol. 119, ed. S. Hartland, pp. 147–193. Marcel Dekker, Inc., New York.

[4] Blokhuis, E.M., Shilkrot, Y., Widom, B., 1995. Young's law with gravity. Molecular Physics 86, 891–899.

[5] Bormashenko, E., 2009. Young, Boruvka-Neumann,Wenzel and CassieBaxter equations as the transversality conditions for the variational problem of wetting. Colloids and Surfaces A: Physicochem. Eng. Aspects 345, 163-165.

[6] Bormashenko, E., Whyman, G., 2008. Variational approach to wetting problems: Calculation of a shape of sessile liquid drop deposited on a solid substrate in external field. Chem. Phys. Letters 463, 103-105.

[7] Boruvka, L., Neumann, A.W., 1977. Generalization of the classical theory of capillarity. J. Chem. Phys. 66, 5464–5476.

[8] Dussan, E.B., 1979. On the spreading of liquids on solid surfaces: static and dynamic contact lines. Ann. Rev. Fluid Mech. 11, 371–400.

[9] Ehrhard, P., Davis, S.H., 1991. Non-isothermal spreading of liquid drops on horizontal plates. J. Fluid Mech. 229, 365–388.

[10] Fan, H., Gao, Y.X., Huang, X.Y., 2001. Thermodynamics modeling for moving contact line in gas/liquid/solid system: Capillary rise problem revisited. Phys. Fluids 13, 1615–1623.

[11] Freund, L.B., 1990. Dynamic Fracture Mechanics. Cambridge University Press, New York.

[12] Gao, Y.X., Fan, H., Xiao, Z., 2000. A thermodynamics model for solder profile evolution Acta Materialia 48, 863–874.

[13] de Gennes, P.G., 1985. Wetting: statics and dynamics. Rev. Modern Phys. 57, 827–863.

[14] de Gennes, P.G., Brochard-Wyart, F., Quéré, D., 2004. Capillarity and Wetting Phenomena. Springer, Berlin.

[15] Gurtin, M.E., 2000. Configurational Forces as Basic Concepts of Continuum Physics. Applied Math. Sciences 137, Springer, New York.

[16] Fan, H., 2006. Liquid droplet spreading with line tension effect. J. Phys: Condens. Matter 18, 4481-4488.

[17] Gibbs, J.W., 1961. Collected Works. Dover, New York.

[18] Hirth, J.P., Lothe, J., 1982. Theory of Dislocations, 2nd ed. McGraw-Hill, New York.

[19] Johnson, R.E., 1959. Conflicts between Gibbsian thermodynamics and recent treatments of interfacial energies in solid-liquid-vapor. J. Phys. Chem. 63, 1655-1658.

[20] Lamb, H., 1932. Hydrodynamics. Chapter XII. Dover.

[21] Li, R., Ashgriz, N., Chandra, S., 2010. Maximum spread of droplet on solid surface: low Reynolds and Weber numbers. J. Fluids Eng. 132, 061302-1–5.

[22] Lubarda, V.A., Talke, K.A., 2011. An analysis of the equilibrium droplet shape based on an ellipsoidal droplet model. Langmuir 27, 10705-10713

[23] Lyttleton, R.A., 1953. The stability of rotating liquid masses. Cambridge Univ. Press.

[24] Maugin, G.A., 1995. Material forces: Concepts and applications. Appl. Mech. Rev. 48, 213–245.

[25] Miller, C.A., Neogi, P., 2008. Interfacial Phenomena. Equilibrium and Dynamic Effects, 2nd ed. CRC Press, Boca Raton, FL.

[26] Padday, J.F., 1969. Theory of surface tension. In: Surface and Colloid Science, Vol. 1, ed. E. Matijevic, pp. 101–151. Wiley, New York.

[27] Padday, J.F., 1991. Capillary in microgravity. In: Capillarity Today. Lecture Notes in Physics, Vol. 386, eds. G. Pétré and A. Sanfeld, pp. 90–107, Springer, New York.

[28] Rowlinson, J.S., Widom, B., 1982. Molecular Theory of Capillarity. Oxford, Clarendon.

[29] Suo, Z., 1997. Motion of microscopic surfaces in materials. Adv. Appl. Mech. 33, 193–294.

[30] Young, T., 1805. An essay on the cohesion of fluids. Philos. Trans. R. Soc. London 95, 65–87.

[31] Whyman, G., Bormashenko, E., Stein, T., 2008. The rigorous derivation of Young, Cassie-Baxter and Wenzel equations and the analysis of the contact angle hysteresis phenomenon. Chem. Phys. Letters 450, 355-359.

[32] Widom, B., 1995. Line tension and the shape of a sessile drop. J. Phys. Chem. 99, 2803–2806.

[33] Zisman, W., 1964. Contact Angle, Wettability and Adhesion – Adv. in Chem. Ser. 43, Amer. Chem. Soc.

Appendix A: Variational analysis with virtual displacements orthogonal to the surface of the droplet

If it is recognized at the outset of the analysis that the specific configurational force is orthogonal to the surface of the droplet, the magnitude of the configurational force f can de derived directly from the variational analysis based on the virtual displacement field δu which is orthogonal to the surface of the droplet, and which satisfies the constraint of constant volume and the non-separation condition ($\delta u = 0$) along the triple-phase contact line (unless the contact angle happens to be $\theta_0 = 90^\circ$, in which case δu along the contact line is tangential to the substrate). The analysis can be conveniently

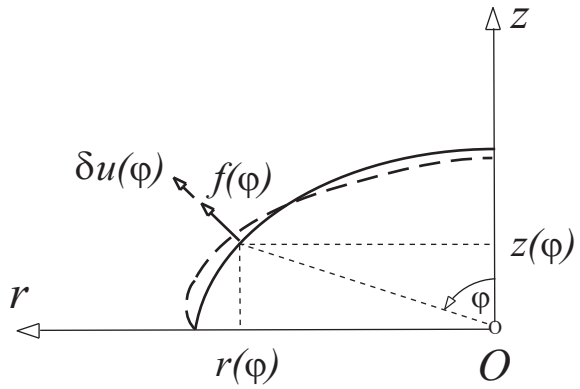

Figure 7: The virtual displacement imposed in the direction orthogonal to the surface of the droplet takes the surface from its solid- to dashed-line configuration. The corresponding configurational force is f.

performed by adopting the parametric representation of the droplet's profile $r = r(\varphi)$ and $z = z(\varphi)$, where the angle $\varphi \in [0, \pi/2]$ is used as a parameter (Fig. 7). The arc length of the droplet's profile is then $\mathrm{d}s = (r'^2 + z'^2)^{1/2}\mathrm{d}\varphi$, while $\mathrm{d}z = z'\mathrm{d}\varphi$, where the superposed prime now designates the derivative with respect to φ. The expressions for the relevant quantities appearing in the potential function expression

$$\Pi = \sigma_{lv}S + (\sigma_{sl} - \sigma_{sv})R^2\pi + 2\pi R\tau + G - K - \lambda V\,, \quad R = r(\pi/2)\,, \quad \text{(A.1)}$$

are

$$S = \int_0^{\pi/2} 2\pi r(r'^2 + z'^2)^{1/2}\,\mathrm{d}\varphi\,, \quad V = -\int_0^{\pi/2} \pi r^2 z'\,\mathrm{d}\varphi\,, \qquad \text{(A.2)}$$

$$G = -\int_0^{\pi/2} (\Delta\gamma)\pi r^2 z z'\,\mathrm{d}\varphi\,, \quad K = -2\pi\int_0^{\pi/2} \mu(r)z'\,\mathrm{d}\varphi\,. \qquad \text{(A.3)}$$

The minus sign in front of the integrals of the expressions for V, G and K appears because, as z runs from 0 to h, the angle φ changes from $\pi/2$ to 0 (i.e., $z' < 0$). In view of (A.1)–(A.3), the potential function Π in (A.1) can be written as

$$\Pi = \int_0^{\pi/2} \tilde{\Phi}(r, z, r', z')\,\mathrm{d}\varphi\,, \qquad \text{(A.4)}$$

where

$$\begin{aligned}\tilde{\Phi} &= 2\pi\sigma_{lv} r (r'^2 + z'^2)^{1/2} + \pi r^2 z' [\lambda - (\Delta\gamma) z] + 2\pi\mu(r) z' \\ &\quad + \left[(\sigma_{sl} - \sigma_{sv})\pi r^2 + 2\pi r\tau\right] \bar{\delta}(\pi/2 - \theta_0)\bar{\delta}(\pi/2 - \varphi)\,.\end{aligned} \tag{A.5}$$

The delta function $\bar{\delta}(\pi/2 - \theta_0)$ multiplies the last term on the right-hand side of (A.5), because the radius $R = r(\pi/2)$ of the solid/liquid contact area is constant under the considered virtual displacement δu (thus the constant term in (A.5) can be omitted), unless the contact angle $\theta_0 = \pi/2$, in which case δu at the contact point is at the same time orthogonal to S and in the direction parallel to the substrate.

The variation of the potential functional $\delta\Pi$, divided by the corresponding infinitesimal variation $\delta u(\psi)$ of the shape function, is

$$\begin{aligned}\frac{\delta\Pi}{\delta u(\psi)} &= \left\{ \left[\frac{\partial\tilde{\Phi}}{\partial r} - \frac{\mathrm{d}}{\mathrm{d}\varphi}\left(\frac{\partial\tilde{\Phi}}{\partial r'}\right)\right]\sin\theta + \left[\frac{\partial\tilde{\Phi}}{\partial z} - \frac{\mathrm{d}}{\mathrm{d}\varphi}\left(\frac{\partial\tilde{\Phi}}{\partial z'}\right)\right]\cos\theta \right\}_{\varphi=\psi} \\ &\quad + \left(\frac{\partial\tilde{\Phi}}{\partial r'}\right)_{\varphi=\pi/2} \bar{\delta}(\pi/2 - \theta_0)\bar{\delta}(\pi/2 - \psi) \\ &\quad - \left(\frac{\partial\tilde{\Phi}}{\partial r'}\sin\theta + \frac{\partial\tilde{\Phi}}{\partial z'}\cos\theta\right)_{\varphi=0} \bar{\delta}(\psi)\,.\end{aligned} \tag{A.6}$$

Due to the orthogonality of δu to the droplet's profile, we used $\delta r = \delta u \sin\theta$ and $\delta z = \delta u \cos\theta$ in the above derivation (Fig. 7). The first two terms on the right-hand side have the usual form of the Euler-Lagrange's differential equation, while the second two terms account for the boundary conditions.

From (A.5) it readily follows that

$$\begin{aligned}\frac{\partial\tilde{\Phi}}{\partial r} &= 2\pi\left[\sigma_{lv}(r'^2 + z'^2)^{1/2} + r z'(\lambda - z\Delta\gamma) + \frac{\partial\mu}{\partial r} z'\right] \\ &\quad + 2\pi\left[(\sigma_{sl} - \sigma_{sv})R + \tau\right]\bar{\delta}(\pi/2 - \theta_0)\bar{\delta}(\pi/2 - \varphi)\,,\end{aligned} \tag{A.7}$$

$$\frac{\partial\tilde{\Phi}}{\partial r'} = 2\pi\sigma_{lv}\frac{r r'}{(r'^2 + z'^2)^{1/2}} = 2\pi r\sigma_{lv}\cos\theta\,, \tag{A.8}$$

$$\frac{\mathrm{d}}{\mathrm{d}\varphi}\left(\frac{\partial\tilde{\Phi}}{\partial r'}\right) = 2\pi\sigma_{lv}\left[(r'^2 + z'^2)^{1/2} - 2r z'\kappa\right], \tag{A.9}$$

and

$$\frac{\partial\tilde{\Phi}}{\partial z} = -(\Delta\gamma)\pi r^2 z' \,, \tag{A.10}$$

$$\begin{aligned} \frac{\partial\tilde{\Phi}}{\partial z'} &= 2\pi\sigma_{lv}\,\frac{rz'}{(r'^2+z'^2)^{1/2}} + \pi r^2(\lambda - z\Delta\gamma) + 2\pi\mu\,, \\ \frac{z'}{(r'^2+z'^2)^{1/2}} &= -\sin\theta\,, \end{aligned} \tag{A.11}$$

$$\frac{\mathrm{d}}{\mathrm{d}\varphi}\left(\frac{\partial\tilde{\Phi}}{\partial z'}\right) = 2\pi r r'(-2\sigma_{lv}\kappa + \lambda) - (\Delta\gamma)\pi r(rz' + 2zr') + 2\pi\,\frac{\partial\mu}{\partial r}\,r' \,. \tag{A.12}$$

The mean curvature of the droplet's surface is $\kappa = (\kappa_1 + \kappa_2)/2$, where

$$\kappa_1 = -\frac{z'}{r(r'^2+z'^2)^{1/2}}\,, \quad \kappa_2 = \frac{z'r'' - r'z''}{(r'^2+z'^2)^{3/2}} \tag{A.13}$$

are its two principal curvatures. Furthermore, in view of (A.8) and (A.11),

$$\begin{aligned} \left(\frac{\partial\tilde{\Phi}}{\partial r'}\right)_{\varphi=\pi/2} &= 2\pi R\sigma_{lv}\cos\theta_0\,, \\ \left(\frac{\partial\tilde{\Phi}}{\partial r'}\,\sin\theta + \frac{\partial\tilde{\Phi}}{\partial z'}\,\cos\theta\right)_{\varphi=0} &= 2\pi\mu(0) = 0\,. \end{aligned} \tag{A.14}$$

Consequently, by substituting (A.7)–(A.14) into (A.6), and noting that $r' = -z'\cot\theta$ and $(z'\sin\theta - r'\cos\theta) = z'/\sin\theta$, we obtain

$$\begin{aligned} \frac{\delta\Pi}{\delta u(\psi)} &= 2\pi r(\psi)\,[-2\sigma_{lv}\kappa(\psi) + \lambda - z(\psi)\Delta\gamma + k(r)]\,\frac{z'(\psi)}{\sin\theta} \\ &\quad + 2\pi R\left(\sigma_{lv}\,\cos\theta_0 + \sigma_{sl} - \sigma_{sv} + \frac{\tau}{R}\right)\bar{\delta}(\pi/2-\theta_0)\bar{\delta}(\pi/2-\psi)\,. \end{aligned} \tag{A.15}$$

The relation $k = r^{-1}\partial\mu/\partial r$ was also used.

If the spreading proceeds to the equilibrium droplet configuration with $\theta_0 = \pi/2$ at an arbitrary stage of spreading, (A.15) reduces to

$$\begin{aligned} \frac{\delta\Pi}{\delta u(\psi)} &= 2\pi r(\psi)\,[-2\sigma_{lv}\kappa(\psi) + \lambda - z(\psi)\Delta\gamma + k(r)]\,\frac{z'(\psi)}{\sin\theta} \\ &\quad + 2\pi R\left(\sigma_{sl} - \sigma_{sv} + \frac{\tau}{R}\right)\bar{\delta}(\pi/2-\psi)\,, \quad \theta_0 = \pi/2\,. \end{aligned} \tag{A.16}$$

Otherwise, (A.15) gives

$$\frac{\delta\Pi}{\delta u(\psi)} = 2\pi r(\psi)\left[-2\sigma_{lv}\kappa(\psi) + \lambda - z(\psi)\Delta\gamma + k(r)\right]\frac{z'(\psi)}{\sin\theta}\,. \tag{A.17}$$

A.1 Configurational forces

Consider first the case $\theta_0 \neq \pi/2$, so that (A.17) applies, and introduce the specific configurational force ($\mathbf{f}$), per unit area of the liquid/vapor interface, such that

$$-\delta\Pi = \int_0^{\pi/2} 2\pi r(\varphi) f(\varphi)\delta u(\varphi)\,\mathrm{d}s\,, \quad \mathrm{d}s = (r'^2 + z'^2)^{1/2}\mathrm{d}\varphi\,. \tag{A.18}$$

By dividing this with the shape variation $\delta u(\psi)$, and recalling that $r' = -z'\cot\theta$, we find

$$\frac{\delta\Pi}{\delta u(\psi)} = 2\pi r(\psi) f(\psi)\,\frac{z'(\psi)}{\sin\theta}\,. \tag{A.19}$$

The comparison of (A.17) and (A.19) yields the expression for the configurational force

$$f(\psi) = -2\sigma_{lv}\kappa(\psi) + \lambda - z(\psi)\Delta\gamma + k(r)\,. \tag{A.20}$$

To determine an expression for the Lagrangian multiplier λ, we note that from the local spherical geometry of the droplet near its apex $\varphi = 0$, the configurational force there must be $f(0) = \Delta p(0) - 2\sigma_{lv}/b$, where $\Delta p(0)$ is the pressure difference across the surface of the droplet at $\varphi = 0$, and b is the local radius of the curvature. Thus,

$$\lambda = \Delta p(0) + h\Delta\gamma\,, \tag{A.21}$$

where h is the height of the droplet. The substitution of (A.21) into (A.20) therefore gives

$$f(\psi) = -2\sigma_{lv}\kappa(\psi) + (\Delta\gamma)[h - z(\psi)] + \Delta p(0) + k(r)\,. \tag{A.22}$$

If $\theta_0 = \pi/2$, so that (A.16) applies at a particular droplet's configuration, (A.18) is replaced with

$$-\delta\Pi = \int_0^{\pi/2} 2\pi r(\varphi) f(\varphi)\delta u(\varphi)\,\mathrm{d}s + 2\pi RF\delta u(\pi/2)\,, \tag{A.23}$$

so that

$$\frac{\delta\Pi}{\delta u(\psi)} = 2\pi r(\psi) f(\psi) \frac{z'(\psi)}{\sin\theta} - 2\pi R F \bar{\delta}(\pi/2 - \psi)\,. \tag{A.24}$$

The comparison of (A.24) and (A.16) yields (A.22) for the configurational force f, and

$$F = \sigma_{sv} - \sigma_{sl} - \frac{\tau}{R} \tag{A.25}$$

for the configurational force per unit length of a three-phase contact line, in agreement with (17) and (47) when $\theta_0 = \pi/2$.

Appendix B: General variational analysis

A more general derivation of the expressions for the specific configurational forces f and F, not committed to a particular coordinate system, is as follows. The potential function for a droplet deposited on a flat surface of the substrate is

$$\Pi = \sigma_{lv} S + (\sigma_{sl} - \sigma_{sv}) A + \tau l + G - K - \lambda V\,, \tag{B.1}$$

where A is the contact area between the droplet and the substrate, and l is the length of the circumference of A, i.e., the length of the three-phase contact line C. If a surface element $\mathrm{d}S$ at an arbitrary point of S, which is not a point of the three-phase contact line, is given a virtual displacement $\delta\mathbf{u} = \delta u \mathbf{m}$, in the direction of the unit vector $\mathbf{m}$, then[4]

$$\delta(\mathrm{d}S) = 2\kappa \delta u_n \,\mathrm{d}S\,. \tag{B.2}$$

The component of $\delta\mathbf{u}$ in the direction $\mathbf{n}$ orthogonal to $\mathrm{d}S$ is $\delta\mathbf{u}_n = \delta u_n \mathbf{n} = \delta u\,(\mathbf{m}\cdot\mathbf{n})\mathbf{n}$. As in the analysis by Suo (1997) and Fan (2005), the surface element at the point of the three-phase contact line needs to be additionally stretched in the direction tangential to the surface by the amount ($\delta\mathbf{u}_t \times$

[4]Indeed, if $\mathrm{d}S$ is expressed in terms of its principal radii of curvature as $\mathrm{d}S = R_1 R_2\,\mathrm{d}\vartheta_1 \mathrm{d}\vartheta_2$, then $\mathrm{d}S + \delta(\mathrm{d}S) = (R_1 + \delta u)(R_2 + \delta u_n)\,\mathrm{d}\vartheta_1 \mathrm{d}\vartheta_2$, so that $\delta(\mathrm{d}S) = (\kappa_1 + \kappa_2)\delta u_n \mathrm{d}S = 2\kappa\delta u_n \mathrm{d}S$, where $\kappa_1 = 1/R_1$ and $\kappa_2 = 1/R_2$ are the principal curvatures, and $\delta u_n = \delta\mathbf{u}\cdot\mathbf{n}$ is the projection of $\delta\mathbf{u}$ onto $\mathbf{n}$. The tangential component of virtual displacement $\delta\mathbf{u}_t = \mathbb{P}\cdot\delta\mathbf{u} = \delta\mathbf{u} - \delta u_n\mathbf{n}$, where $\mathbb{P} = \mathbb{I} - \mathbf{n}\otimes\mathbf{n}$ is the projection operator, does not alter $\mathrm{d}S$. The two-dimensional identity tensor over the surface S is denoted by $\mathbb{I} = \mathbf{t}_1\otimes\mathbf{t}_1 + \mathbf{t}_2\otimes\mathbf{t}_2$, where $\mathbf{t}_1$ and $\mathbf{t}_2$ are its tangent vectors, and $\otimes$ denotes the dyadic product.

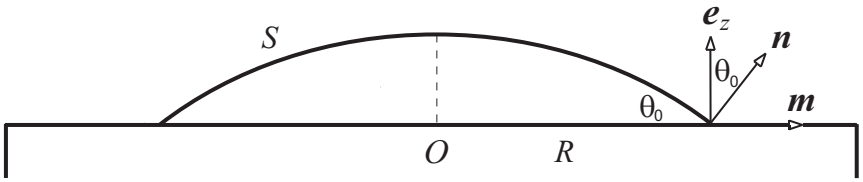

Figure 8: The equilibrium droplet's configuration with the wetting contact angle θ_0. The unit normal orthogonal to the surface of the droplet along the three-phase contact circle is $\mathbf{n}$. The unit vector $\mathbf{m}$ is in the plane of the substrate, orthogonal to the contact circle, while $\mathbf{e}_z$ is the unit vector orthogonal to the substrate.

$\mathrm{d}\boldsymbol{l}) \cdot \mathbf{n}$, to preserve the droplet's contact with the substrate (after $\mathrm{d}S$ has expanded by the normal component $\delta\mathbf{u}_n$ of the total (horizontal) virtual displacement $\delta\mathbf{u}$ at the contact point (Fig.8). The infinitesimal arc length along the contact line in the positive (counterclockwise) direction is $\mathrm{d}l$. Since $\delta\mathbf{u}_t = \delta u\mathbf{m} - \delta u_n\mathbf{n}$, we have $(\delta\mathbf{u}_t \times \mathrm{d}\boldsymbol{l}) \cdot \mathbf{n} = \delta u(\mathbf{m} \times \mathrm{d}\boldsymbol{l}) \cdot \mathbf{n} = \delta u(\mathbf{e}_z \cdot \mathbf{n})\mathrm{d}l$. Consequently, the total area change of the surface element along the contact line can be expressed as

$$\delta(\mathrm{d}S) = 2\kappa\delta u_n \,\mathrm{d}S + \cos\theta_0 \,\delta u \,\mathrm{d}l. \tag{B.3}$$

In view of this, and the Reynolds transport theorem

$$\delta \int_V \eta \,\mathrm{d}V = \int_V \delta\eta \,\mathrm{d}V + \int_S \eta\delta u_n \,\mathrm{d}S\,, \tag{B.4}$$

where η is a scalar field defined within the volume V, we can write

$$\begin{aligned}
&\delta S = \int_S 2\kappa\delta u_n \,\mathrm{d}S + \oint_C \cos\theta_0 \,\delta u \,\mathrm{d}l, \quad \delta V = \int_S \delta u_n \,\mathrm{d}S\,,\\
&\delta A = \oint_C \delta u \,\mathrm{d}l, \quad \delta l = \oint_C \frac{\delta u}{R} \,\mathrm{d}l,\\
&\delta G = \int_S (\Delta\gamma) z\delta u_n \,\mathrm{d}S\,, \quad \delta K = \int_S k\delta u_n \,\mathrm{d}S\,.
\end{aligned} \tag{B.5}$$

The radius of curvature of the contact circle C is denoted by R. Consequently, the variation of the potential function (B.1), associated with an infinitesimal displacement field δu over S, such that δu is horizontal along

the triple-phase contact line (preserving the droplet's contact with the substrate), is

$$\delta\Pi = \int_S (2\sigma_{lv}\kappa + z\Delta\gamma - k - \lambda)\delta u_n \,\mathrm{d}S + \oint_C \left(\sigma_{lv}\cos\theta_0 + \sigma_{sl} - \sigma_{sv} + \frac{\tau}{R}\right)\delta u \,\mathrm{d}l\,. \tag{B.6}$$

The specific configurational force $\mathbf{f} = f\mathbf{n}$, per unit area of S, and the configurational force $\mathbf{F} = F\mathbf{m}$, per unit length of the three-phase contact line C, are defined such that

$$-\delta\Pi = \int_S \mathbf{f}\cdot\delta\mathbf{u}\,\mathrm{d}S + \oint_C \mathbf{F}\cdot\delta\mathbf{u}\mathrm{d}l. \tag{B.7}$$

Since $\mathbf{f}\cdot\delta\mathbf{u} = f\delta u_n$ and $\mathbf{F}\cdot\delta\mathbf{u} = F\delta u$, equation (B.7) becomes

$$-\delta\Pi = \int_S f\delta u_n \,\mathrm{d}S + \oint_C F\delta u \,\mathrm{d}l\,. \tag{B.8}$$

The comparison of (B.6) and (B.8) therefore yields

$$f = -2\sigma_{lv}\kappa - z\Delta\gamma + k + \lambda\,, \tag{B.9}$$

in agreement with (A.20), and

$$F = \sigma_{sv} - \sigma_{sl} - \sigma_{lv}\cos\theta_0 - \frac{\tau}{R}\,, \tag{B.10}$$

in agreement with (47). The condition of constant volume is additionally imposed in the numerical evaluation of the droplet's shape at each stage of its spreading, which specifies the Lagrangian multiplier λ appearing in (B.9).

Submitted in June 2011

Konfiguracione sile i ravnotežni oblik rotirajuće kapljice na čvrstoj ravnoj podlozi

Ravnotežni oblik rotirajuće kapljice na ravnoj podlozi u polju gravitacije je odredjen numeričkim rešenjem nelinearne diferencijalne jednačine, uz korišćenje odgovarajuće iterativne procedure. Nelinearna diferencijalna jednačina i njeni granični uslovi su izvedeni varijacionom analizom, koja daje analitičke izraze za konfiguracione sile na površini kapljice i uzduž linije kontakta izmedju kapljice, čvrste podloge i gasnog okruženja. Dokazano je da je specifična konfiguraciona sila u pravcu normale na površ kapljice. Kvalitativni i kvantitativni uticaj ugaone brzine na ravnotežni oblik kapljice je diskutovan.

doi:10.2298/TAM1201027L Math.Subj.Class.: 76E99, 80A20, 81U30, 76S05